Heliyon 10 (2024) e37850

Contents lists available at ScienceDirect

Heliyon

journal homepage: www.cell.com/heliyon

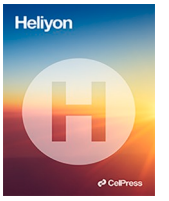

Research article

A pilot pharmacokinetic and Metabolite identification study of Erinacine A in a Single landrace pig model

Ying-Yu Chen [a,1], Ting-Wei Lin [a,1], I-Chen Li [a], Lin Tsung [b], Chun-Hsiang Hou [b], Chi-Yu Yang [b], Tsung-Ju Li [a,*], Chin-Chu Chen [a,c,d,e,**]

[a] *Biotech Research Institute, Grape King Bio Ltd., Taoyuan 325, Taiwan*
[b] *GLP Animal Laboratory, Agricultural Technology Research Institute, Hsinchu 300, Taiwan*
[c] *Institute of Food Science and Technology, National Taiwan University, Taipei 106, Taiwan*
[d] *Department of Bioscience Technology, Chung Yuan Christian University, Taoyuan 320, Taiwan*
[e] *Department of Food Science, Nutrition and Nutraceutical Biotechnology, Shih Chien University, Taipei 104, Taiwan*

ARTICLE INFO

Keywords:
Erinacine A
Erinacine B
Landrace pig
Nerve growth factor
Blood-brain barrier
Pharmacokinetic
Metabolite

ABSTRACT

Erinacine A has been proven to have the ability to protect nerves and have the benefit of neurohealth. However, the pharmacokinetic and metabolites study of erinacine A in pigs, whose physiology and anatomy are similar to humans, have not been reported. In this study, 5 mg/kg of erinacine A was intravenously administered to the landrace pig. Blood, cerebrospinal fluid, and brain tissue samples were collected and analyzed by HPLC-QQQ/MS and UPLC-QTOF/MS. The results indicated the following pharmacokinetic parameters in plasma samples: with an area under the plasma concentration versus time curve (AUC) were 38.02 ± 0.03 mg•min/L ($AUC_{0\text{-}60}$) and 43.60 ± 0.06 mg•min/L ($AUC_{0\text{-}\infty}$), clearance (CL) was 0.11 ± 0.00 L/min•kg, volume of distribution (V_d) was 4.24 ± 0.00 L/kg, and terminal half-life ($T_{1/2\beta}$) was 20.85 ± 0.03 min. In the cerebrospinal fluid samples, erinacine A was detected after 15 min and the highest concentration (5.26 ± 0.58 μg/L) was observed at 30 min. In the brain tissue sample, 77.45 ± 0.58 μg/L of erinacine A was found. In the study of metabolites, there were 6 identical metabolites in plasma and brain tissue. To our surprise, erinacine B was found to be the metabolite of erinacine A, and its concentration increased over time as erinacine A was metabolized. In summary, this study is the first to demonstrate that erinacine A can be found in the cerebrospinal fluid of landrace pigs. Additionally, the metabolite identification of erinacine A in landrace pigs is also investigated.

1. Introduction

Erinacines, which are isolated from *Hericium erinaceus* mycelia, are natural products with cyathin diterpenoid as a core structure. Most erinacines have been reported to have the ability to induce the synthesis of nerve growth factor (NGF) and have the benefit of protecting nerve [1–4]. Among erinacines, erinacine A not only can stimulate the synthesis of nerve growth factor but also increase catecholamine content in the central nervous system of rats [5]. In the light of this, there is an increasing amount of research studies on

* Corresponding author.
** Corresponding author. Biotech Research Institute, Grape King Bio Ltd., Taoyuan 325, Taiwan.
E-mail addresses: tsungju.li@grapeking.com.tw (T.-J. Li), gkbioeng@grapeking.com.tw (C.-C. Chen).
[1] These authors contributed equally to work.

https://doi.org/10.1016/j.heliyon.2024.e37850
Received 19 February 2024; Received in revised form 29 August 2024; Accepted 11 September 2024
Available online 11 September 2024

the impact of erinacine A on neurohealth.

In addition to neuroprotection [6–9], erinacine A can also ameliorate neurodegenerative diseases [10–12] and possess anti-aging [13–15], anti-cancer [16], anti-oxidant [17], and anti-depression [18]. In the latest study, Hsu et al. reported that erinacine A can protect retinal ganglion cell morphometry and retain the visual function of traumatic optic neuropathy in the optic nerves crushed rat model by suppressing apoptosis, neuroinflammation, and oxidative stress [19].

Bioavailability, tissue distribution, and protein binding of erinacine A in Sprague-Dawley rats have been reported in previous studies [20]. The results showed that the absolute bioavailability of erinacine A was 24.39 %. In the tissue distribution experiment, erinacine A was observed in eight organs including stomach, small intestine, large intestine, liver, heart, lung, kidney, and brain. Moreover, this study is the first time to prove that erinacine A can penetrate the blood-brain barrier of rats by passive diffusion. However, there is currently no animal experimental model with physiology and anatomy similar to that of humans to confirm whether erinacine A is capable of penetrating the blood-brain barrier.

Compared with other established animal models, pigs have similarities to humans with regard to genetics, anatomy, physiology, and biochemistry including the cardiovascular system, gastrointestinal tract, liver, adrenals, skin, and kidney [21–23]. Because of these features, minipigs, as a non-rodent model, have been used for regulatory toxicity testing nowadays [24]. Moreover, pigs as an animal model in pharmacokinetic studies of potential drugs have been reported, such as anti-bacterial [25–28], anti-virus [29], anti-cancer [30], pediatric drug [31], inner ear drug [32], and so on. Apart from small molecules, macromolecules are also investigated in pharmacokinetic studies in pigs' model [33,34].

In this study, the landrace pig was used as an animal model to examine the pharmacokinetics and metabolites of erinacine A. Erinacine A was intravenously administered to the landrace pig. Blood and cerebrospinal fluid samples were collected at various time points. These samples were quantified by HPLC-QQQ/MS. Metabolites of plasma samples were identified by UPLC-QTOF/MS. Finally, after the landrace pig was sacrificed, erinacine A and its metabolites were quantified and identified in the brain tissue sample.

2. Materials and methods

2.1. Materials and reagents

Hericium erinaceus strain (BCRC 35669) was obtained from the Bioresources Collection and Research Center in Food Industry Research and Development Institute, Hsinchu, Taiwan. Ammonium acetate solution (BioUltra, for molecular biology, ~5 M in H_2O) was obtained from Merck (Darmstadt, Germany); acetonitrile (LC-MS grade) and formic acid (FA, LC-MS grade, 98 % purity) were obtained from Honeywell (Honeywell Burdick and Jackson, Muskegon, MI, USA).

2.2. Preparation of erinacine A

The *Hericium erinaceus* strain was first grown in an ager slant before being transferred to a potato dextrose ager plate at 26 °C for 15 days. After 15 days, the *Hericium erinaceus* cultures were transferred to 2-L flasks containing 1.3 L of liquid medium. The liquid culture was shaken at 120 rev/min 25 °C for 5 days. Then the flasks were scaled up to 500-L and 20-ton fermenters for 5 days and 12 days, respectively. The pH of the culture medium is 4.5 and contains 4.5 % glucose, 0.5 % soybean powder, 0.25 % yeast extract, 0.25 % peptone, and 0.05 % $MgSO_4$. Finally, the *Hericium erinaceus* mycelia were harvested at the end of the 20-ton fermentation process. These raw materials were lyophilized, grounded in powder, and stored in a desiccator. Erinacine A was then extracted from the *Hericium erinaceus* mycelia containing 5 mg/g and purified through column chromatography to obtain purity of 99 % [35].

2.3. Animals

The care of the landrace pig and the experimental protocols used in this study were approved by the Institutional Animal Care and Use Committee of Agricultural Technology Research Institute, Hsinchu, Taiwan (IACUC#111022). The landrace pig was housed in a controllable breeding room. The room temperature was maintained at 18–26 (±2) °C and relative humidity was between 30 and 70 % with a 12-h light and dark cycle.

2.4. Pharmacokinetic study

Erinacine A was dissolved in DMSO and diluted in PBS. When the landrace pig weight about 120 kg, the drug solutions were intravenous injection to ear vein at a dose of 5 mg/kg. Blood and cerebrospinal fluid samples were collected prior to treatment administration (0 min) and at 5, 15, 30, 60 min. Blood samples were collected into K2 EDTA blood collection tubes (BD) and thoroughly mixed for 10 min. Subsequently, the samples were centrifuged at 1811×*g* for 15 min. The supernatant was collected and stored at −30 °C. Cerebrospinal fluid samples were collected from the landrace pig with the aid of X-ray imaging to ensure precise localization. A lumbar puncture needle was then inserted to the appropriate depth for cerebrospinal fluid collection. The cerebrospinal fluid was directly aspirated through the needle. After collection, the samples were immediately stored at −30 °C. For sample preparation, the plasma (100 μL) or cerebrospinal fluid (100 μL) was mixed with 400 μL of acetonitrile. The mixture was vortexed and centrifuged at 13,523×*g* for 10 min. The supernatant was collected and ready for used. The concentration of erinacine A in plasma and cerebrospinal fluid were quantified by high-performance liquid chromatography/triple quadrupole mass spectrometry (HPLC-QQQ/MS).

2.5. Metabolic study

Blood samples' preparation was mentioned as above. For the brain tissue sample, the landrace pig was sacrificed after sampling at 60 min. After euthanized and exsanguinated the landrace pig, a small portion of brain tissue was sampled using an 8 mm biopsy punch and stored at −30 °C immediately. For sample preparation, the brain tissue sample was washed by 0.9 % NaCl before homogenization. Then, the homogenates (100 μL) were mixed with 400 μL of acetonitrile. The mixture was vortexed and centrifuged at 13,523×*g* for 10 min. The supernatant was collected and ready for used. The metabolites of blood samples and the brain tissue sample were identified by ultra-performance liquid chromatography/quadrupole time-of-flight mass spectrometry (UPLC-QTOF/MS).

2.6. HPLC-QQQ/MS analysis

High-performance liquid chromatography/triple quadrupole mass spectrometry (HPLC-QQQ/MS) for quantitative analysis of erinacine A was performed on an Agilent 1100 series HPLC system (Agilent, Waldbronn, Germany) coupled with an API 3000 triple quadrupole mass spectrometer (Applied Biosystems, Concord, Ontario, Canada). A turbo ionspray electrospray ionization (ESI) interface in positive ionization mode was used. Chromatographic separation was carried out in an Agilent Eclipse XDB-C18 (3.5 μm, 4.6 × 100 mm). The column temperature was maintained at 22 °C. The mobile phase consisted of water (A) and acetonitrile (B) with gradient elution as follows: 0 min, 70 % B; 0–5 min, 70–100 % B; 5–8 min, 100%B; 8–8.1 min, 100-70 % B; 8.1–11 min, 70 % B. The flow rate was 350 μL/min and injection volume was 10 μL. Mass spectrometric detection was conducted in multiple reaction monitoring (MRM) mode with parameters as follows: ion source voltage, +4500V; ion source temperature, 350 °C; nebulizer gas, 8 psi; curtain gas, 7 psi; collision gas, 7 psi; dwell time, 200 ms. The specific precursor to product ion transitions of erinacine A is 433.2 → 301.2. Data analysis was performed with Analyst 1.4.2 software (Applied Biosystems, Concord, ON, Canada). The analysis method of HPLC-QQQ/MS has been reported in previous studies [20,36].

2.7. UPLC-QTOF/MS analysis

Ultra-performance liquid chromatography/quadrupole time-of-flight mass spectrometry (UPLC-QTOF/MS) for erinacine A's metabolites identification was performed on an Agilent 1290 Inifinity II UPLC system (Agilent, Palo Alto, CA, USA) coupled with an Agilent 6546 quadrupole time-of-flight mass spectrometer (Agilent, Palo Alto, CA, USA) which equipped with an electrospray ionization (ESI) source. Chromatographic separation was carried out in a Phenomenex Kinetex C18 LC Column (1.7 μm, 3.0 × 100 mm). The column temperature was maintained at 40 °C. The mobile phase A consisted of water with 0.1 % (v/v) formic acid in positive mode, 0.1 % (v/v) formic acid and 10 mM ammonium acetate in negative mode. The mobile phase B was acetonitrile. The gradient elution with a 3-min post-time was as follows: 0–0.5 min, 5 % B; 0.5–1 min, 5–20 % B; 1–6 min, 20–50 % B; 6–16 min, 50–100 % B; 16–22 min, 100 % B. The flow rate was 400 μL/min and injection volume was 2 μL. Mass spectrometric detection was conducted in multiple reaction monitoring (MRM) mode with parameters as follows: ion source voltage (ESI^+/ESI^-), +4000V/-3000V; gas temperature, 320 °C; drying gas flow rate, 8 L/min; nebulizer pressure, 45 psi; sheath gas temperature, 350 °C; sheath gas flow rate. 12 L/min; collision energy, 10, 20, 40, 60 V. Metabolites were identified using Agilent MassHunter Biotransformation software (version B.04.00) (Santa Clara CA, USA). Chromatograms and mass spectra of the parent and identified metabolites were extracted using Agilent MassHunter Qualitative Analysis software (version B.05.00) (Santa Clara, CA, USA). The analysis method of UPLC-QTOF/MS has been reported in previous studies [36].

2.8. Data analysis

All experimental data were presented as mean ± standard deviation (STD) of triplicate measurements. Elimination rate constant (k_{el}) was derived from the regression equation of plasma concentration versus time curve of erinacine A. The area under the plasma

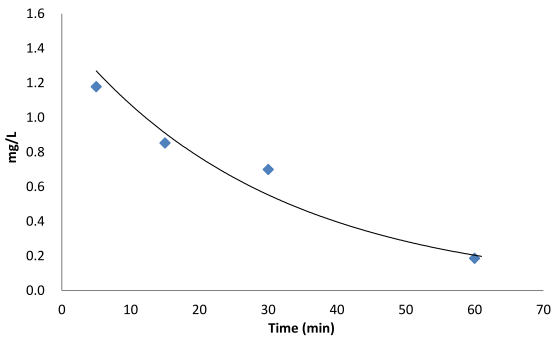

Fig. 1. Plasma concentration versus time curve of erinacine A in the landrace pig after intravenous administration of erinacine A at 5 mg kg^{-1} BW.

concentration versus time curve of erinacine A (AUC) was calculated by the trapezoidal method. Terminal half-life ($T_{1/2\beta}$), clearance (CL), and volume of distribution (V_d) were calculated by equation $0.693/k_{el}$, dose/$AUC_{0-\infty}$ and dose/C_5 respectively.

3. Results and discussion

3.1. Pharmacokinetic of erinacine A in blood samples

Erinacine A in blood samples at different time points were quantified by HPLC-QQQ/MS. The results were shown in Fig. 1. Blood sample at 0 min was also analyzed and erinacine A was not observed before landrace pig was intravenously administered (data not shown). According to the regression equation, elimination rate constant (k_{el}) was 0.033 ± 0.00. Terminal half-life ($T_{1/2\beta}$), AUC_{0-60}, $AUC_{0-\infty}$, clearance (CL), and volume of distribution (V_d) were calculated by the equation mentioned in Section 2.7, and the results were 20.85 ± 0.03 min, 38.02 ± 0.03 mg•min/L, 43.60 ± 0.06 mg•min/L, 0.11 ± 0.00 L/kg/min, and 4.24 ± 0.00 L/kg respectively. These pharmacokinetic parameters were summarized in Table 1. However, only one pig was treated in this study, so the data should be seen as preliminary.

We compared erinacine A with other central nervous drugs, which were also intravenously administered to the pigs, and summarized the pharmacokinetic parameters in Table 2. The terminal half-life of erinacine A in blood was shorter than other central nervous drugs. It was only 8 min longer than Δ9-tetrahydrocannabinol (THC). The results showed that the time of metabolic process in blood of erinacine A was faster than other central nervous drugs. Besides, the clearance of erinacine A was the highest. Aarati Rai et al. reported that pig's weight and clearance had a positive correlation when intravenously administered the same dose of morphine to the different weight of piglets [37]. In other words, the clearance was higher when the piglet was heavier. Based on this result, 120 kg of landrace pig studied in this research was the heaviest, so the clearance is the highest was predictable. Furthermore, we observed that the longer of the terminal half-life, the lower of the clearance. We also observed that the volume of distribution of erinacine A was the highest which means erinacine A was prior to leaving the plasma and entering the extravascular compartments (interstitial compartment) of the body. As a non-polar molecule, erinacine A has a tendency for lipid solubility, which allows for easier diffusion through plasma.

3.2. Quantification of erinacine a in cerebrospinal fluid samples and brain tissue

Erinacine A in cerebrospinal fluid samples at different time points and the brain tissue sample were quantified by HPLC-QQQ/MS. According to the results, erinacine A entered into the cerebrospinal fluid at about 10 min (Fig. 2). The highest concentration of erinacine A was observed at 30 min, which was 5.26 ± 0.58 μg/L (Table 3). After that, erinacine A was decreased over time. In the brain tissue sample, 77.45 ± 0.58 μg/L of erinacine A was found (Table 3).

The central nervous system (CNS) in brain is not only protected by the meninges but also protected by blood-meningeal barrier (BMB), blood-brain barrier (BBB), and blood-cerebrospinal fluid (CSF) barrier (BCB) [42]. If the molecules want to enter the microenvironment of brain, they must pass through these natural barriers. Among of them, after the drugs pass through the blood-brain barrier, they will cross the ependymal or across the pia-glial membranes at the surface of the brain and spinal cord and then get into cerebrospinal fluid [43].

Tsai et al. have been reported that erinacine A is observed in the brain tissue of Sprague-Dawley rats after oral administration of 2.381 g/kg BW of *Hericium erinaceus* mycelia extract (equivalent to 50 mg/kg BW of erinacine A) to the rats [20]. In addition, they also demonstrate that erinacine A can penetrate the blood-brain barrier by passive diffusion for the first time. However, there is no further evidence to prove that erinacine A could get into the cerebrospinal fluid after it passed through the blood-brain barrier.

For this study, it is the first to observe that erinacine A was found in cerebrospinal fluid and brain tissue of landrace pigs. The results showed that erinacine A indeed crossed the blood-brain barrier and entered into the cerebrospinal fluid by following route. After 5 mg/kg BW of erinacine A was intravenously administered to the landrace pig, erinacine A would first penetrate the blood-brain barrier to the brain tissue. Then, it would get into cerebrospinal fluid by passing through the ependymal or the pia-glial membranes at the surface of the brain and spinal cord.

Table 1
Pharmacokinetic Parameters of erinacine A in the landrace pig after intravenous administration of erinacine A at 5 mg kg^{-1} BW.

PK Parameters	Intravenous	Unit
k_{el}	0.033 ± 0.00	–
$T_{1/2\beta}$	20.85 ± 0.03	min
AUC_{0-60}	38.02 ± 0.03	mg·min·L^{-1}
$AUC_{0-\infty}$	43.60 ± 0.06	mg·min·L^{-1}
CL	0.11 ± 0.00	L·kg^{-1}·min^{-1}
V_d	4.24 ± 0.00	L·kg^{-1}

Table 2
Pharmacokinetic study of erinacine A compared with central nervous system drugs in pigs.

Drug	Breed	Body weight (kg)	Dose (mg·kg^{-1})	$T_{1/2\beta}$ (min)	CL (mL·kg^{-1}·min^{-1})	V_d (L·kg^{-1})	Reference
erinacine A	Landrace	120	5	21	115	4.24	This study
amoxycillin	Landrace x Large White	78–82	20	203	5	1.07	[38]
Δ^9-tetrahydrocannabinol	Swabian Hall male	47.7 (mean)	0.2	13	43	0.30	[39]
deoxynivalenol	Yorkshire	20–26	1	66	–	1.13	[40]
Lidocaine	Landrace	1–2.5	2	160	4	0.74	[41]

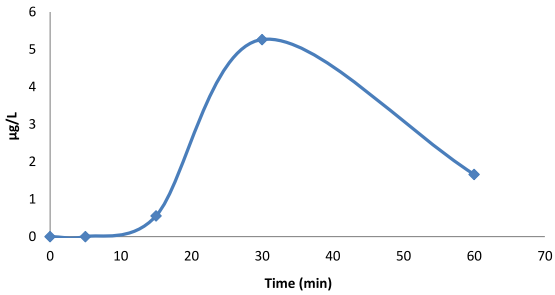

Fig. 2. Cerebrospinal fluid concentration versus time curve of erinacine A in the landrace pig after intravenous administration of erinacine A at 5 mg/kg BW.

Table 3
Concentration of erinacine A in cerebrospinal fluid samples and brain tissue after intra-venous administration of erinacine A at 5 mg/kg BW.

Time (min)	Cerebrospinal fluid (μg/L)	Brain tissue (μg/L)
5	0.00	–
15	0.56	–
30	5.26	–
60	1.66	–
sacrificed	–	77.45

Data expressed as means.

3.3. Metabolites identification of erinacine A

The metabolites of erinacine A in blood and brain tissue were identified by UPLC-QTOF/MS. The results were shown in Table 4. There were found 24 metabolites (assigned as M1-M24) and 6 of them were also found in brain tissue. The identical metabolites in blood and brain tissue were M1 (alcohols dehydration), M2 (demethylation), M8 (glycine conjugation), M14 (2x hydroxylation and sulfation), M17 (hetero oxide reduction + hydrogenation), and M23 (demethylation + oxidation + glucuronidation). In other words, in addition to erinacine A, these 6 metabolites (M1, M2, M8, M14, M17, M23) also could enter into the brain tissue. In our previous study, liver metabolites of erinacine A in rat and human liver S9 have been already identified [36]-. Compared with that, M1 (alcohols dehydration), M2 (demethylation), and M3 (2x hydroxylation) were also identified in rat and human liver S9 (Table S1). These 3 metabolites (M1, M2, M3) may be metabolized by pig liver S9.

To our surprise, erinacine B (M24) was one of the metabolites of erinacine A. Erinacine B, which is one of the compounds in *Hericium erinaceus*, also affects stimulating synthesis of nerve growth factor [44,45]. Due to the identical molecular weight of erinacine A and erinacine B, it is not possible to differentiate these two compounds based on MS results alone. However, the use of MS/MS fragments proves instrumental in identifying compounds with the same molecular weight. Table 4 and Fig. 3 showcase the MS/MS fragments and spectrum of erinacine A and erinacine B, respectively. Based on the MS/MS results, the primary fragment of erinacine A was measured at 283.2055 (Fig. 3 (a)), while erinacine B was found to be 135.1170 (Fig. 3 (b)). It is worth noting that 283.2065 was the second highest fragment observed for erinacine B. Therefore, the major MS/MS fragment enables us to differentiate between erinacine A and erinacine B. Besides, global natural products social molecular networking (GNPS) [46] showed the correlation between erinacine A and erinacine B (Fig. S1). The third evidence was that the concentration of erinacine B increased over time as erinacine A was metabolized (Fig. 4). Based on the evidence provided, it can be concluded that erinacine B is indeed a metabolite of erinacine A. However, erinacine B had not been detected in cerebrospinal fluid and brain tissue samples. Further investigation is needed by increasing the number of animals to understand how erinacine B circulates in biological systems.

Table 4
Metabolites of erinacine A in plasma and brain.

ID	Metabolic reaction	Formula	Exact mass	Accurate mass	Mass error (ppm)	Fragment	Plasma	Brain
parent	Erinacine A	$C_{25}H_{36}O_6$	432.2516	432.2512	0.9	171.1166, 199.1478, 255.2104, 283.2055[a], 301.2162	✓	✓
M1	Alcohols Dehydration	$C_{25}H_{34}O_5$	414.2427	414.2406	2.95	119.0859[a], 135.0808, 147.0656, 281.1397, 415.2491	✓	✓
M2	Demethylation	$C_{25}H_{34}O_6$	418.2357	418.2355	0.33	59.0136[a], 61.9883, 107.0366, 300.0919, 329.0945	✓	✓
M3	2x Hydroxylation	$C_{25}H_{36}O_8$	464.2423	464.2410	2.75	57.0322, 119.0852, 181.0998, 209.0956, 295.9762[a]	✓	
M4	3x Hydroxylation	$C_{25}H_{36}O_9$	480.2357	480.2359	−0.41	61.9878[a], 199.0814, 282.8705, 394.9423, 534.0104	✓	
M5	2x Hydrogenation	$C_{25}H_{40}O_6$	436.2821	436.2825	−0.95	61.9883, 75.0089, 146.9665, 343.9977, 495.2958[a]	✓	
M6	Decarboxylation	$C_{24}H_{36}O_4$	388.2600	388.2614	−3.41	81.0694, 105.0699[a], 107.0862, 119.0861, 159.1162	✓	
M7	Phosphorylation	$C_{25}H_{37}O_9P$	512.2199	512.2175	4.66	61.9881[a], 211.1131, 255.1029, 448.3075, 511.52126	✓	
M8	Glycine Conjugation	$C_{27}H_{39}NO_7$	489.2721	489.2727	−1.15	76.0757[a], 119.0857, 281.1371, 415.2117, 490.2796	✓	✓
M9	Glutamine Conjugation	$C_{30}H_{44}NO_8$	546.3072	546.3067	0.98	61.9882[a], 89.0245, 504.3039, 528.3087, 605.3212	✓	
M10	Glucuronide Conjugation	$C_{31}H_{44}O_{12}$	608.2805	608.2833	−4.55	70.0652[a], 129.1022, 286.1379, 293.0972, 347.0118	✓	
M11	2x Sulfate Conjugation	$C_{25}H_{36}O_{12}S_2$	592.1658	592.1648	1.62	258.0061, 277.0455, 343.9966[a], 459.0009, 507.9302	✓	
M12	Ethyl to Carboxylic Acid	$C_{24}H_{32}O_8$	448.2103	448.2097	1.31	81.0686[a], 85.0655, 151.0738, 177.0198, 185.0105	✓	
M13	Hydroxylation + Glucuronide	$C_{31}H_{44}O_{13}$	624.2775	624.2782	−1.07	59.0133, 75.0088, 89.0242, 475.2342[a], 623.2704	✓	
M14	2x Hydroxylation and Sulfation	$C_{25}H_{36}O_{14}S_2$	624.1540	624.1547	−1.06	70.0651[a], 72.0808, 86.0966, 110.0712, 197.1306	✓	✓
M15	Hydrolysis + 2x Oxidation	$C_{25}H_{38}O_9$	482.2517	482.2516	0.31	61.9886, 71.0139, 146.9677, 201.0225, 541.2658[a]	✓	
M16	Decarboxylation and Glucuronidation	$C_{30}H_{44}O_{11}$	580.2876	580.2884	−1.39	59.0140, 75.0080, 113.0238, 475.2333[a], 625.2858	✓	
M17	Hetero oxide reduction + Hydrogenation	$C_{25}H_{38}O_5$	418.2690	418.2719	−3.12	57.0692, 86.0968[a], 102.0915, 124.9982, 163.0148	✓	✓
M18	Carboxylation + Glucuronidation	$C_{31}H_{42}O_{14}$	638.2578	638.2575	0.53	265.1586, 277.1589, 295.1700, 313.1806[a], 331.1906	✓	
M19	Oxidation + Acetylcysteination	$C_{30}H_{45}NO_{10}S$	611.2751	611.2764	−2.15	61.9877, 146.9654, 157.9712, 174.9555[a], 337.0002	✓	
M20	2x Oxidation + Glucuronidation	$C_{31}H_{44}O_{14}$	640.2736	640.2731	0.82	83.0492, 157.1011, 239.1433, 279.1741, 297.1848[a]	✓	
M21	Glucuronidation + Hydrogenation	$C_{31}H_{46}O_{12}$	610.2986	610.2989	−0.53	61.9885, 75.0082, 283.2061, 459.2397[a], 609.2913	✓	
M22	Gluthation Conjugation + Hydroxylation	$C_{35}H_{51}N_3O_{13}S$	753.3113	753.3143	−3.88	70.0650, 72.0805, 86.0966, 270.1820, 623.8371[a]	✓	
M23	Demethylation + Oxidation + Glucuronidation	$C_{30}H_{42}O_{13}$	610.2616	610.2625	−1.47	146.9652, 343.9979, 487.1938, 505.2089, 655.2598[a]	✓	✓
M24	Erinacine B	$C_{25}H_{36}O_6$	432.2515	432.2512	0.72	135.1170[a], 149.1321, 183.1164, 253.1948, 283.2065	✓	

[a] Most abundance peak of MS/MS fragments.

4. Conclusions

This is the first study to discuss pharmacokinetics and metabolites of erinacine A in landrace pigs, whose genetics, anatomy, physiology, and biochemistry are considered close to humans. According to the pharmacokinetic parameters of landrace pig after intravenous administration of erinacine A at 5 mg kg^{-1} BW, the terminal half-life of erinacine A in plasma was only 21 min. However, the volume of distribution of erinacine A is higher than other central nervous system drugs. This may be because erinacine A has better lipid solubility and, therefore leaves plasma more easily. This also echoes the reason for the short half-life in plasma. Apart from blood samples, erinacine A also observed in cerebrospinal fluid and brain tissue samples. After erinacine A entered into brain tissue by crossing the blood-brain barrier, it passed through the ependymal or the pia-glial membranes at the surface of the brain and spinal cord

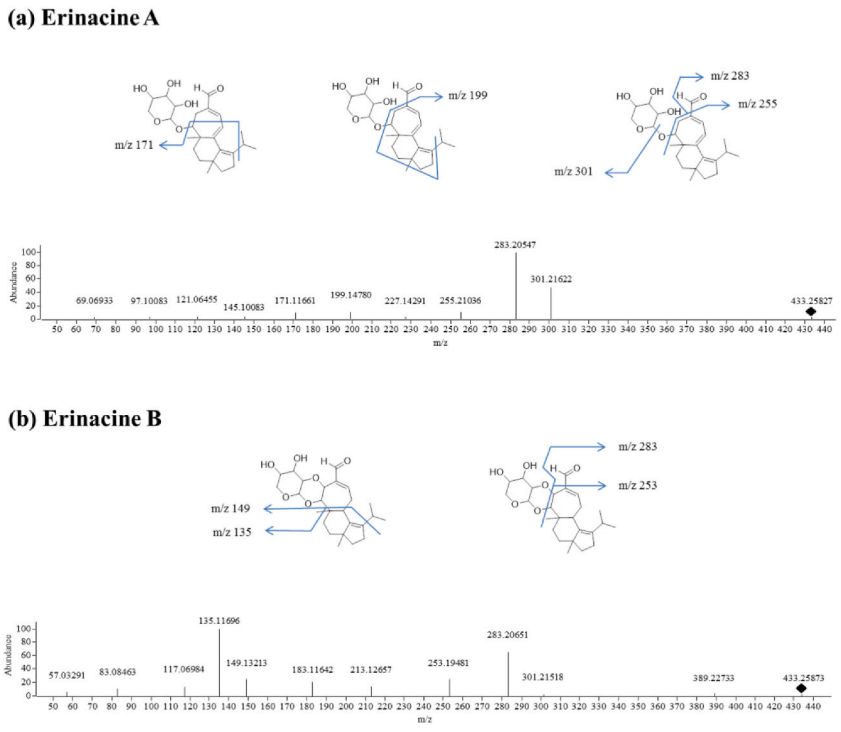

Fig. 3. The MS/MS spectrum of erinacine A (a) and erinacine B (b).

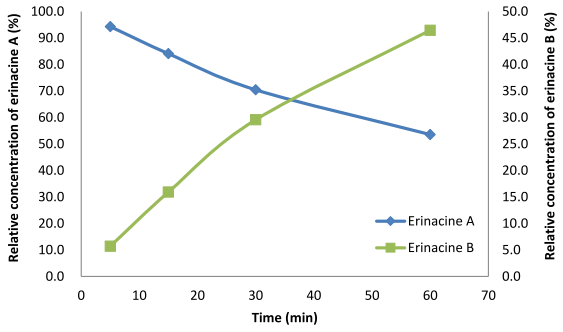

Fig. 4. Relative concentration versus time curve of erinacine A and erinacine B in plasma after intravenous administration of erinacine A at 5 mg/kg BW in landrace pig.

and get into cerebrospinal fluid. This is further evidence to show that erinacine A could penetrate the blood-brain barrier.

In the experiment of metabolites identification, there were 24 metabolites in plasma and 6 of them were identical in brain tissue. Among these 24 metabolites, M1 (alcohols dehydration), M2 (demethylation), and M3 (2x hydroxylation) may be metabolized by pig liver S9. In addition, there were three methods used to confirm that erinacine B, which can stimulate the growth of nerve growth factor, was the metabolite of erinacine A. The first method involved analyzing the major MS/MS fragment of erinacine A and erinacine B. The second method was the GNPS analysis of erinacine A and its metabolites. The last method involved studying the correlation between erinacine A and erinacine B during the metabolism of erinacine A. However, erinacine B was not been found in brain tissue. Whether erinacine B can enter into brain tissue still needs further investigation.

In summary, this pilot study is the first to investigate the pharmacokinetics and metabolites of erinacine A in landrace pigs. The results showed that erinacine A has a shorter terminal half-life compared with other central nervous drugs, which were intravenously administered to the pigs. However, clearance and volume of distribution of erinacine A were the highest. This study is also the first to observe erinacine A in cerebrospinal fluid and brain tissue in a non-rodent model. The findings indicated that erinacine A was able to cross the blood-brain barrier and enter the cerebrospinal fluid. Additionally, erinacine B was identified as one of the metabolites of erinacine A.

Ethics statement

The care of the landrace pig and the experimental procedures used in this study were authorized by the Institutional Animal Care and Use Committee of Agricultural Technology Research Institute, Hsinchu, Taiwan. The ethics approval number for this study is IACUC#111022.

Data availability statement

The raw materials and compounds presented in this study are available from the corresponding author upon reasonable request.

CRediT authorship contribution statement

Ying-Yu Chen: Writing – review & editing, Writing – original draft, Visualization, Formal analysis, Data curation. **Ting-Wei Lin:** Writing – review & editing, Writing – original draft, Project administration, Methodology, Formal analysis, Data curation. **I-Chen Li:** Visualization. **Lin Tsung:** Methodology. **Chun-Hsiang Hou:** Methodology. **Chi-Yu Yang:** Methodology. **Tsung-Ju Li:** Writing – review & editing, Project administration, Investigation, Conceptualization. **Chin-Chu Chen:** Writing – review & editing, Supervision, Resources, Investigation, Funding acquisition, Conceptualization.

Declaration of competing interest

The authors declare the following financial interests/personal relationships which may be considered as potential competing interests:Ying-Yu Chen, Ting-Wei Lin, I-Chen Li, Tsung-Ju Li, Chin-Chu Chen reports a relationship with Grape King Bio Ltd that includes: employment. Lin Tsung, Chun-Hsiang Hou, Chi-Yu Yang reports a relationship with Agricultural Technology Research Institute that includes: employment. If there are other authors, they declare that they have no known competing financial interests or personal relationships that could have appeared to influence the work reported in this paper.

Acknowledgment

Graphical abstract was created with BioRender.com.

Appendix B. Supplementary data

Supplementary data to this article can be found online at https://doi.org/10.1016/j.heliyon.2024.e37850.

References

[1] H. Kawagishi, C. Zhuang, R. Yunoki, Compounds for dementia from Hericium erinaceum, Drugs Future 33 (2008) 149, https://doi.org/10.1358/dof.2008.033.02.1173290.
[2] P.L. Lai, M. Naidu, V. Sabaratnam, K.H. Wong, R.P. David, U.R. Kuppusamy, N. Abdullah, S.N.A. Malek, Neurotrophic properties of the Lion's mane medicinal mushroom, Hericium erinaceus (Higher Basidiomycetes) from Malaysia, Int. J. Med. Mushrooms 15 (2013) 539–554, https://doi.org/10.1615/intjmedmushr.v15.i6.30.
[3] I.C. Li, L.Y. Lee, T.T. Tzeng, W.P. Chen, Y.P. Chen, Y.J. Shiao, C.C. Chen, Neurohealth properties of Hericium erinaceus mycelia enriched with erinacines, Behav. Neurol. (2018) 5802632, https://doi.org/10.1155/2018/5802634.
[4] J. Wei, J.y. Li, X.l. Feng, Y. Zhang, X. Hu, H. Hui, X. Xue, J. Qi, Unprecedented neoverrucosane and cyathane diterpenoids with anti-neuroinflammatory activity from cultures of the culinary-medicinal mushroom Hericium erinaceus, Molecules 28 (2023) 6380, https://doi.org/10.3390/molecules28176380.
[5] M. Shimbo, H. Kawagishi, H. Yokogoshi, Erinacine A increases catecholamine and nerve growth factor content in the central nervous system of rats, Nutr. Res. 25 (2005) 617–623, https://doi.org/10.1016/j.nutres.2005.06.001.
[6] K.F. Lee, J.H. Chen, C.C. Teng, C.H. Shen, M.C. Hsieh, C.C. Lu, K.C. Lee, L.Y. Lee, W.P. Chen, C.C. Chen, Protective effects of Hericium erinaceus mycelium and its isolated erinacine A against ischemia-injury-induced neuronal cell death via the inhibition of iNOS/p38 MAPK and nitrotyrosine, Int. J. Mol. Sci. 15 (2014) 15073–15089, https://doi.org/10.3390/ijms150915073.
[7] H.T. Huang, C.H. Ho, H.Y. Sung, L.Y. Lee, W.P. Chen, Y.W. Chen, C.C. Chen, C.S. Yang, S.F. Tzeng, Hericium erinaceus mycelium and its small bioactive compounds promote oligodendrocyte maturation with an increase in myelin basic protein, Sci. Rep. 11 (2021) 6551, https://doi.org/10.1038/s41598-021-88168-w.
[8] S.L. Lee, J.Y. Hsu, T.C. Chen, C.C. Huang, T.Y. Wu, T.Y. Chin, Erinacine a prevents lipopolysaccharide-mediated glial cell activation to protect dopaminergic neurons against inflammatory factor-induced cell death in vitro and in vivo, Int. J. Mol. Sci. 23 (2022) 810, https://doi.org/10.3390/ijms23020810.
[9] P.C. Hsu, Y.J. Lan, C.C. Chen, L.Y. Lee, W.P. Chen, Y.C. Wang, Y.H. Lee, Erinacine A attenuates glutamate transporter 1 downregulation and protects against ischemic brain injury, Life Sci. 306 (2022) 120833, https://doi.org/10.1016/j.lfs.2022.120833.
[10] T.T. Tzeng, C.C. Chen, L.Y. Lee, W.P. Chen, C.K. Lu, C.C. Shen, C.Y. Huang F, C.C. Chen, Y.-J. Shiao, Erinacine A-enriched Hericium erinaceus mycelium ameliorates Alzheimer's disease-related pathologies in APPswe/PS1dE9 transgenic mice, J. Biomed. Sci. 23 (2016) 49, https://doi.org/10.1186/s12929-016-0266-z.
[11] I.C. Li, H.H. Chang, C.H. Lin, W.P. Chen, T.H. Lu, L.Y. Lee, Y.W. Chen, Y.-P. Chen, C.C. Chen, D.P.C. Lin, Prevention of early Alzheimer's disease by erinacine A-enriched Hericium erinaceus mycelia pilot double-blind placebo-controlled study, Front. Aging Neurosci. 12 (2020) 155, https://doi.org/10.3389/fnagi.2020.00155.

[12] K.F. Lee, S.Y. Tung, C.C. Teng, C.H. Shen, M.C. Hsieh, C.Y. Huang, K.C. Lee, L.Y. Lee, W.P. Chen, C.C. Chen, Post-treatment with erinacine A, a derived diterpenoid of H. erinaceus, attenuates neurotoxicity in MPTP model of Parkinson's disease, Antioxidants 9 (2020) 137, https://doi.org/10.3390/antiox9020137.
[13] I.C. Li, L.Y. Lee, Y.J. Chen, M.Y. Chou, M.F. Wang, W.P. Chen, Y.P. Chen, C.C. Chen, Erinacine A-enriched Hericium erinaceus mycelia promotes longevity in Drosophila melanogaster and aged mice, PLoS One 14 (2019) e0217226, https://doi.org/10.1371/journal.pone.0217226.
[14] L.Y. Lee, W. Chou, W.P. Chen, M.F. Wang, Y.J. Chen, C.C. Chen, K.C. Tung, Erinacine a-enriched hericium erinaceus mycelium delays progression of age-related cognitive decline in senescence accelerated mouse prone 8 (samp8) mice, Nutrients 13 (2021) 3659, https://doi.org/10.3390/nu13103659.
[15] Y.C. Chan, T.C. Lin, C.C. Chen, L.Y. Lee, W.P. Chen, Y.Z. Liu, J.H. Hwang, Effects of erinacine A-enriched Hericium erinaceus on elderly hearing-impaired patients: a double-blind, randomized, placebo-controlled clinical trial, J. Funct.Foods 97 (2022) 105220, https://doi.org/10.1016/j.jff.2022.105220.
[16] P. Prasher, M. Sharma, A.K. Sharma, J. Sharifi-Rad, D. Calina, C. Hano, W.C. Cho, Key oncologic pathways inhibited by Erinacine A: a perspective for its development as an anticancer molecule, Biomed. Pharmacother. 160 (2023) 114332, https://doi.org/10.1016/j.biopha.2023.114332.
[17] C.H. Hsu, E.C. Liao, W.C. Chiang, K.L. Wang, Antioxidative activities of micronized solid-state cultivated hericium erinaceus rich in erinacine A against MPTP-induced damages, Molecules 28 (2023) 3386, https://doi.org/10.3390/molecules28083386.
[18] C.H. Chiu, C.C. Chyau, C.C. Chen, L.Y. Lee, W.P. Chen, J.L. Liu, W.H. Lin, M.C. Mong, Erinacine A-enriched Hericium erinaceus mycelium produces antidepressant-like effects through modulating BDNF/PI3K/Akt/GSK-3β signaling in mice, Int. J. Mol. Sci. 19 (2018) 341, https://doi.org/10.3390/ijms19020341.
[19] C.L. Hsu, Y.T. Wen, T.C. Hsu, C.C. Chen, L.Y. Lee, W.P. Chen, R.K. Tsai, Neuroprotective effects of erinacine A on an experimental model of traumatic optic neuropathy, Int. J. Mol. Sci. 24 (2023) 1504, https://doi.org/10.3390/ijms24021504.
[20] P.C. Tsai, Y.K. Wu, J.H. Hu, I.C. Li, T.W. Lin, C.C. Chen, C.F. Kuo, Preclinical bioavailability, tissue distribution, and protein binding studies of erinacine A, a bioactive compound from Hericium erinaceus mycelia using validated LC-MS/MS method, Molecules 16 (2021) 4510, https://doi.org/10.3390/molecules26154510.
[21] L.B. Schook, T.V. Collares, K.A. Darfour-Oduro, A.K. De, L.A. Rund, K.M. Schachtschneider, F.K. Seixas, Unraveling the swine genome: implications for human health, Annu. Rev. Anim. Biosci. 3 (2015) 219–244, https://doi.org/10.1146/annurev-animal-022114-110815.
[22] H. Tang, M. Mayersohn, Porcine prediction of pharmacokinetic parameters in people: a pig in a poke? Drug Metab. Dispos. 46 (2018) 1712–1724, https://doi.org/10.1124/dmd.118.083311.
[23] M.M. Swindle, A. Makin, A.J. Herron, F.J. Clubb Jr., K.S. Frazier, Swine as models in biomedical research and toxicology testing, Vet. Pathol. 49 (2012) 344–356, https://doi.org/10.1177/0300985811402846.
[24] G. Bode, P. Clausing, F. Gervais, J. Loegsted, J. Luft, V. Nogues, J. Sims, The utility of the minipig as an animal model in regulatory toxicology, J. Pharmacol. Toxicol. Methods 62 (2010) 196–220, https://doi.org/10.1016/j.vascn.2010.05.009.
[25] E. Eckhardt, Y. Li, S. Mamerow, J. Schinköthe, J. Sehl-Ewert, J. Dreisbach, B. Corleis, A. Dorhoi, J. Teifke, C. Menge, Pharmacokinetics and efficacy of the benzothiazinone BTZ-043 against tuberculous mycobacteria inside granulomas in the Guinea pig model, Antimicrob. Agents Chemother. 67 (2023) e01438, https://doi.org/10.1128/aac.01438-22.
[26] Z. Somogyi, P. Mag, R. Simon, Á. Kerek, P. Szabó, E. Albert, I. Biksi, Á. Jerzsele, Pharmacokinetics and pharmacodynamics of florfenicol in plasma and synovial fluid of pigs at a dose of 30 mg/kgbw following intramuscular administration, Antibiotics 12 (2023) 758, https://doi.org/10.3390/antibiotics12040758.
[27] S.B. Yeshwante, P. Hanafin, B.K. Miller, L. Rank, S. Murcia, C. Xander, A. Annis, V.K. Baxter, E.J. Anderson, B. Jermain, R. Konicki, A.A. Schmalstig, I. Stewart, M. Braunstein, A.J. Hickey, G.G. Rao, Pharmacokinetic considerations for optimizing inhaled spray-dried pyrazinoic acid formulations, Mol. Pharm. 20 (2023) 4491–4504, https://doi.org/10.1021/acs.molpharmaceut.3c00199.
[28] D. Yi, X. Wen, W. Xu, Y. Xu, X. Deng, G. Yan, L. Wu, Q. Liang, Z. Liang, J. Peng, Development of an amoxicillin-radix scutellaria extract formulation and evaluation of its pharmacokinetics in pigs, BMC Vet. Res. 19 (2023) 164, https://doi.org/10.1186/s12917-023-03713-1.
[29] G. Schwagerle, M.J. Sharp, A. Parr, D. Schimek, S.I. Mautner, T. Birngruber, Detailed pharmacokinetic characterization of advanced topical acyclovir formulations with IVPT and in vivo Open Flow Microperfusion, Int. J. Pharm. 643 (2023) 123269, https://doi.org/10.1016/j.ijpharm.2023.123269.
[30] F. Requejo, J. Opezzo, A. Vater, M. Asprea, E. Lagomarsino, C. Sampor, A. Fandiño, G. Chantada, J.H. Francis, D.H. Abramson, Pharmacokinetics of orbital topotecan after ophthalmic artery chemosurgery and intravenous infusion in the swine model, Invest. Ophthalmol. Vis. Sci. 64 (2023) 3, https://doi.org/10.1167/iovs.64.12.3.
[31] M. Ayuso, L. Buyssens, M. Stroe, A. Valenzuela, K. Allegaert, A. Smits, P. Annaert, A. Mulder, S. Carpentier, C. Van Ginneken, The neonatal and juvenile pig in pediatric drug discovery and development, Pharmaceutics 13 (2020) 44, https://doi.org/10.3390/pharmaceutics13010044.
[32] E. Yildiz, A.J. Gadenstaetter, M. Gerlitz, L.D. Landegger, R. Liepins, M. Nieratschker, R. Glueckert, H. Staecker, C. Honeder, C. Arnoldner, Investigation of inner ear drug delivery with a cochlear catheter in piglets as a representative model for human cochlear pharmacokinetics, Front. Pharmacol. 14 (2023) 1062379, https://doi.org/10.3389/fphar.2023.1062379.
[33] Y. Zheng, D.B. Tesar, L. Benincosa, et al., Minipig as a potential translatable model for monoclonal antibody pharmacokinetics after intravenous and subcutaneous administration, mAbs 4 (2012) 243–255, https://doi.org/10.4161/mabs.4.2.19387.
[34] K.M. Pedersen, A.K.J. Gradel, T.P. Ludvigsen, B.Ø. Christoffersen, C.A. Fuglsang-Damgaard, K.M. Bendtsen, S.H. Madsen, V. Manfé, H.H.F. Refsgaard, Optimization of pig models for translation of subcutaneous pharmacokinetics of therapeutic proteins: liraglutide, insulin aspart and insulin detemir, Transl. Res. 239 (2022) 71–84, https://doi.org/10.1016/j.trsl.2021.08.005.
[35] I.C. Li, Y.L. Chen, W.P. Chen, L.Y. Lee, Y.T. Tsai, C.C. Chen, C.S. Chen, Genotoxicity profile of erinacine A-enriched Hericium erinaceus mycelium, Toxicol Rep 1 (2014) 1195–1201, https://doi.org/10.1016/j.toxrep.2014.11.009.
[36] Y.H. Kuo, T.W. Lin, J.Y. Lin, Y.W. Chen, T.J. Li, C.C. Chen, Identification of common liver metabolites of the natural bioactive compound erinacine A, purified from Hericium erinaceus mycelium, Appl. Sci. 12 (2022) 1201, https://doi.org/10.3390/app12031201.
[37] A. Rai, S. Bhalla, S.S. Rebello, H. Kastrissios, A. Gulati, Disposition of morphine in plasma and cerebrospinal fluid varies during neonatal development in pigs, J. Pharm. Pharmacol. 57 (2005) 981–985, https://doi.org/10.1211/0022357056505.
[38] M.R. Martinez-Larranaga, A. Anadón, M.A. Martinez, M.J. Diaz, M.T. Frejo, V.J. Castellano, G. Isea, C.O. De la Cruz, Pharmacokinetics of amoxycillin and the rate of depletion of its residues in pigs, Vet. Rec. 154 (2004) 627–632, https://doi.org/10.1136/vr.154.20.627.
[39] N. Schaefer, J.G. Wojtyniak, M. Kettner, J. Schlote, M.W. Laschke, A.H. Ewald, T. Lehr, M.D. Menger, H.H. Maurer, P.H. Schmidt, Pharmacokinetics of (synthetic) cannabinoids in pigs and their relevance for clinical and forensic toxicology, Toxicol. Lett. 253 (2016) 7–16, https://doi.org/10.1016/j.toxlet.2016.04.021.
[40] D. Prelusky, K. Hartin, H. Trenholm, Distribution of deoxynivalenol in cerebral spinal fluid following administration to swine and sheep, J. Environ. Sci. Health. B 25 (1990) 395–413, https://doi.org/10.1080/03601239009372697.
[41] S. Satas, S.I. Johannessen, N.O. Hoem, K. Haaland, D.R. Sorensen, M. Thoresen, Lidocaine pharmacokinetics and toxicity in newborn pigs, Anesth. Analg. 85 (1997) 306–312, https://doi.org/10.1097/00000539-199708000-00012.
[42] K. Alves de Lima, J. Rustenhoven, J. Kipnis, Meningeal immunity and its function in maintenance of the central nervous system in health and disease, Annu. Rev. Immunol. 38 (2020) 597–620, https://doi.org/10.1146/annurev-immunol-102319-103410.
[43] R. Nau, F. Sorgel, H. Eiffert, Penetration of drugs through the blood-cerebrospinal fluid/blood-brain barrier for treatment of central nervous system infections, Clin. Microbiol. Rev. 23 (2010) 858–883, https://doi.org/10.1128/cmr.00007-10.
[44] H. Kawagishi, A. Shimada, R. Shirai, K. Okamoto, F. Ojima, H. Sakamoto, Y. Ishiguro, S. Furukawa, A. Erinacines, B and C, strong stimulators of nerve growth factor (NGF)-synthesis, from the mycelia of Hericium erinaceum, Tetrahedron Lett. 35 (1994) 1569–1572, https://doi.org/10.1016/S0040-4039(00)76760-8.
[45] Z. Rupcic, M. Rascher, S. Kanaki, R.W. Köster, M. Stadler, K. Wittstein, Two new cyathane diterpenoids from mycelial cultures of the medicinal mushroom Hericium erinaceus and the rare species, Hericium flagellum, Int. J. Mol. Sci. 19 (2018) 740, https://doi.org/10.3390/ijms19030740.
[46] M. Wang, J.J. Carver, V.V. Phelan, et al., Sharing and community curation of mass spectrometry data with global natural products social molecular networking, Nat. Biotechnol. 34 (2016) 828–837, https://doi.org/10.1038/nbt.3597.